Published in final edited form as:
J Biophotonics. 2009 October ; 2(10): 573–580. doi:10.1002/jbio.200810071.

Effect of Temperature on Permeation of Low Density Lipoprotein Particles through Human Carotid Artery Tissues

Mohamad G. Ghosn[1], **Michael Leba**[1], **Astha Vijayananda**[1], **Panteha Rezaee**[1], **Joel D. Morrisett**[2], and **Kirill V. Larin**[1]

[1]Biomedical Engineering Program, University of Houston, Houston, Texas USA

[2]Department of Medicine, Baylor College of Medicine, Houston, Texas, USA

Abstract

Quantification of the diffusion of small molecules and large lipid transporting lipoproteins across arterial tissues could be useful in elucidating the mechanism(s) of atherosclerosis. Optical Coherence Tomography (OCT) was used to determine the effect of temperature on the rate of diffusion of glucose and low density lipoproteins (LDL) in human carotid endarterectomy tissue *in vitro*. The permeability rate for glucose was calculated to be (3.51 ± 0.27) $\times 10^{-5}$ cm/sec (n=13) at 20°C, and (3.70 ± 0.44) $\times 10^{-5}$ cm/sec (n=5) at 37°C; for LDL the rate was (2.42 ± 0.33) $\times 10^{-5}$ cm/sec (n=5) at 20°C and (4.77 ± 0.48) $\times 10^{-5}$ cm/sec (n=7) at 37°C, where n is the number of samples. These results demonstrate that temperature does not significantly influence permeation of small molecules (e.g. glucose), however, raising the temperature does significantly increase the permeation of LDL. These results provide new information about the capacity of an atherogenic lipoprotein to traverse the intimal layer of the artery. These results also demonstrate the potential of OCT for elucidating the dynamics of lipoprotein perfusion across the arterial wall.

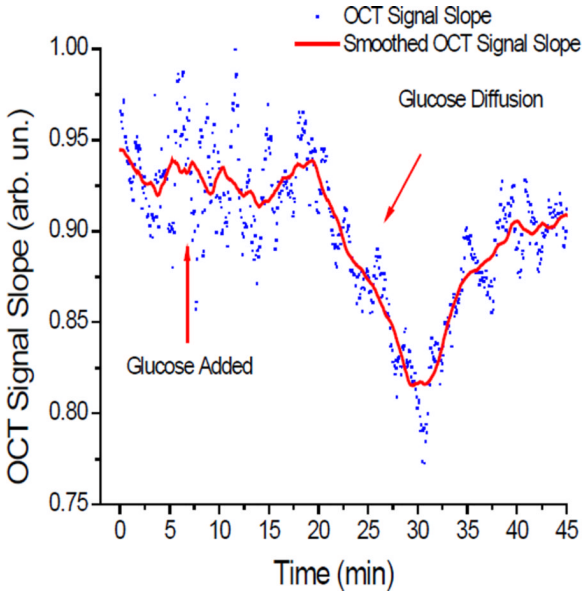

Sample OCT Signal Slope graph recorded during a glucose diffusion experiment at 37°C Ghosn et. al.: Using OCT to quantify effect of temperature on permeation through arterial tissues

Correspondence: K.V. Larin, klarin@uh.edu, Telephone: 713 743 4623, Fax: 713 743 4623.

Keywords

Atherosclerosis; Optical Coherence Tomography; permeability rate; low density lipoproteins

1. Introduction

Atherosclerosis is a chronic inflammatory disease affecting the arterial blood vessels throughout the body and is the major underlying cause of cardiovascular disease [1–3]. The atherosclerotic process typically begins with inflammation of the artery wall, followed by adherence of monocytes which extravigate across the wall and become macrophages. A subsequent step in the process involves permeation of cholesterol transporting lipoproteins such as LDL and Lp[a] across the wall into the subintimal space where they become oxidized and subsequently taken up by macrophages which become cholesterol–laden foam cells [3]. In the esterified form, cholesterol is not easily removed from subintimal lesions, but in the unesterified form, cholesterol can be taken up by HDL particles which exit the artery wall, re-enter the blood stream, and travel to the liver, leading to reverse cholesterol transport. The difference between the amount of cholesterol brought into the arterial wall by LDL and the amount taken out by HDL determines the net cholesterol accumulation in the wall [4–6]. Continual net accumulation causes artery narrowing, reduces blood flow, and increases blood pressure. Arterial inflammation is often attended by focal increased temperature which can lead to increased permeability of lipoproteins. The relative rates at which LDL and HDL permeate the artery wall may play a significant role in determining the rate of progression and regression of atherosclerosis [7]. Thus, it is instructive to examine the wall susceptibility to permeation of low and high molecular weight substances. This vital information can provide further understanding of lipoprotein movement in the arterial wall.

Several methods and techniques have been previously employed to study diffusion processes in tissues. For instance, diffusion of glucose molecules in rabbit sclera was estimated using reflection spectroscopy [8]. The diffusion coefficients for water and glucose were elucidated from Monte-Carlo (MC) numerical simulation method of experimentally measured optical clearing of the tissue. While power of this method has been demonstrated in relatively homogeneous tissues, it might be difficult to estimate diffusion coefficients in multilayered structures without prior known information of tissues layers. Magnetic resonance imaging has proven to be a powerful tool in imaging and estimating the distribution of drugs in an eye globe [9, 10]. However, the need of paramagnetic drugs for such studies and associated relative high cost might limit its routine use. Ultrasound has also been utilized in trans-dermal diffusion studies [11], but low resolution and the need for contact procedure limit its applications. On the other hand, Optical Coherence Tomography (OCT), a relatively novel imaging modality, presents a technique that overcomes limitations posed by the above mentioned methods. OCT offers greater resolution (up to a few micrometers) and may be used noninvasively. Therefore, OCT was employed in this study to quantify the molecular diffusion through arterial tissue. Detailed description of the OCT imaging system and principles of signal generation could be found in several books and reviews [12–16].

Recently, we developed an OCT method for noninvasive assessment of the molecular diffusion in epithelial tissues including the sclera, cornea, skin, and vasculature [17–23]. Because of OCT's ultra-high resolution and ability to reach deep tissue layers (up to a few mm), it is well suited for measuring the permeation of LDL in biological tissues. Accordingly, the objective of this study was to measure changes in LDL and glucose permeation in human carotid endarterectomy tissues *in vitro* under temperatures of 20° C and 37° C.

2. Materials and Methods

Instrumentation

To quantify the permeability of 20% glucose and LDL in normal human carotid tissue, a time-domain OCT system (Imalux Corp. Cleveland, OH) was used. The optical source of this OCT system is a low-coherence, near-infrared broadband laser diode (Superlum Inc., Russia) with a wavelength of 1310 ± 15 nm, and an output power of 3 mW. A schematic of the OCT system utilized is illustrated in Figure 1. The system's scanning functionality was conducted with an endoscopic probe using a single-mode optical fiber for scanning along the x-axis. Piezoelectric modulation of the fiber length enabled scanning in-depth along the z-axis. A two-dimensional (2D) image with dimensions 2.2 × 2.4 mm is obtained every 3 seconds continuously, corresponding to each complete scan both laterally and in-depth. These 2D images were then laterally averaged (over ~1 mm) for speckle noise suppression, producing a single one-dimensional (1D) curve on a logarithmic scale.

Low density lipoproteins

LDL were isolated by sequential ultracentrifugation as described previously [24], and dialyzed via PBS then concentrated by ultrafiltration (Amicon). The stock solution of LDL had a protein concentration of 37.8 mg/ml. An aliquot (100 μl) of the stock solution was added to each well containing a tissue disk and 100 μl PBS, giving a final LDL concentration of 18.9 mg/ml.

Arterial Tissue

Carotid endarterectomy (CEA) tissues were resected at surgery and transferred to PBS at 5 °C. Tissue discs (5mm diameter) were cut with a hole borer (Sargent, Inc) and transferred to a 96 well (6mm diameter well) microtitre plate (Becton Dickinson) with the intimal surface facing up then covered with 100 μl PBS. Relatively normal tissue discs were cut from the proximal common segment and distal external segment, while atherosclerotic tissue disks were cut from the proximal internal and bifurcation segments. One tissue disk was used for each OCT measurement which was started within 6 hr after tissue acquisition. Before initiating a measurement, the tissue disk was transferred to a microtitre plate well containing the permeating species (e.g. glucose or LDL) equilibrated at 20 or 37 °C.

Data acquisition

The sample was imaged in 100 μl of PBS for 5 minutes to acquire baseline data. The 100 μl of PBS was sufficient to totally immerse the tissue; thereby maintaining its hydration condition (Figure 3). 100 μl of the permeating species (40% glucose or 39 mg/ml LDL) was then added to the well, giving a final concentration of 20% sucrose or 19.5 mg/ml LDL. The sample was then imaged for another 40 minutes. Figure 2 illustrates the 2-dimensional image and 1-dimensional graph of the tissue as it was imaged by OCT. Multiple independent experiments for 20% glucose and ~19.5 mg/ml LDL at both 20°C and 37°C were performed.

Data Analysis

The OCT signal slope method (OCTSS) was used to calculate the permeability rate ($\bar{P}$) of glucose and LDL as they travelled through the carotid tissue by measuring changes in the OCT signal as described by us previously [17, 20]. A similar method has also been used to measure glucose concentration level in the blood [25, 26]. For OCT signal analysis, a linear region with minimal fluctuation was selected and its thickness (z_{region}) was measured. The diffusion of glucose through this selected region correlated with changes in the signal slope captured by the OCT system from the resulting scattering changes. As glucose diffuses into the tissue and/or water diffuses out due to osmotic changes, optical changes, such as

refractive index matching, can occur. These changes produce alterations in the slopes as seen in the OCTSS graphs in Figure 4. The time required for the permeating species to move through the selected region (t_{region}) was recorded and the average permeability rate was calculated by dividing the thickness by the time $\bar{P}=\frac{z_{region}}{t_{region}}$.

3. Results and Discussion

A baseline was established for the first five minutes of each experiment using only PBS after which the permeating species was added and its permeation quantified Fig. 4a,b. The permeability rate of 20% glucose was determined to be $(3.51 \pm 0.27) \times 10^{-5}$ cm/sec (n = 13) at 20°C and $(3.70 \pm 0.44) \times 10^{-5}$ cm/sec (n = 5) at 37°C. In contrast, the permeability rate for LDL was found to be $(2.42 \pm 0.33) \times 10^{-5}$ cm/sec (n = 5) at 20°C and $(4.77 \pm 0.48) \times 10^{-5}$ cm/sec (n = 7) at 37°C. Figure 4 illustrates the typical OCTSS graphs of glucose permeation at 20°C and 37°C (Fig. 4a,b) and LDL permeation at 20°C and 37°C (Fig. 4c,d) in human carotid tissue, respectively. As shown by the data above, there is a significant difference between glucose and LDL permeability rates with increased temperature. The permeability rate nearly doubled for LDL whereas glucose did not show any significant change in the permeability rate at the higher temperature (Figure 5). This may be explained by the fact that glucose (Mr = 180) is significantly smaller in size than LDL ($Mr = 2\times10^6$). The increase in permeability rate of LDL beyond that of glucose may indicate a separate transport mechanism for LDL that may be insignificant for small molecules [27]. Surprisingly, at the physiological temperature of 37°C, the larger LDL, permeated faster (1.3-fold) through the arterial tissue than glucose.

Prior studies have shown that the diffusion of molecules into the arterial wall is dependent on the wall permeability of the solute concentration [17, 28]. Permeation in the arterial wall is also influenced by several other factors such as cell death, wounding of endothelial cell membranes, variations in shear stress at branch sites of arteries, dysfunction of the intact endothelial layers, and blood pressure. Temperature also plays a central role in molecular diffusion in biological tissues as confirmed by the results of this study. Several studies have shown an enhanced diffusion rate in biological tissues with an increase in temperature. One such study using human cadaver skin demonstrated an increased permeability rate of hydrophilic Calcein from 25°C to 315°C. That increase was attributed to the disordering of the stratum corneum lipid structure, the disruption of the keratin network structure in the stratum corneum, and the decomposition and vaporization of keratin at high temperatures [29].

Similarly, heat causes the permeability of arteries to increase by affecting the arterial structure. LDL enters the arterial wall as intact particles by vesicular ferrying through endothelial cells and by passive sieving through the pores that are in or between the endothelial cells [30]. In investigation of the transport of LDL through the arterial endothelium in rat aorta and coronary artery, the receptor-mediated process that involved vesicles decreased at lower temperatures which caused a decrease in the permeability of the artery [31].

Another study examining the effect of temperature and hydrostatic pressure on LDL transport across microvessels using quantitative fluorescence microscopy reported a large reduction in LDL permeability rates when microvessels were cooled down. As a result of cooling the microvessels from 18–21 °C to 4–6 °C, the permeability rate of LDL decreased about 80.9 %. The temperature decrease causes closure of the hydraulic pathway and transcellular vesicular pathways of LDL diffusion which decreases its permeability rate [32].

In addition to the aforementioned relationships between permeability rate, temperature and tissue collagen organization, there may be additional factors that may have an influential impact on the permeability rate of the analytes. For example, introduction of chemical compounds with different osmotic properties may alter the scattering of the tissue due to several biophysical mechanisms such as refractive index matching and dehydration [25, 33–36]. The dynamic optical properties of tissues are defined by a multi-flux concept which is composed of the movement of the chemical agent into the tissue and the movement of bulk water out. The two fluxes can either be independent or dependent of each other, contingent on their relative interaction. The diffusion of these agents could be reliant on these and other factors that need to be investigated. We have recently explored one of these factors and found nonlinearity between permeability rate and concentration of the applied agent suggesting strong interaction of the two (at least) fluxes (the movement of the chemical agent into the tissue and the movement of bulk water out) [28]. Therefore, to study the permeability coefficient of certain analytes, more experimental investigations and theoretical models are to be implemented in order to understand the influence of multi- and bidirectional flows in tissues.

4. Conclusion

The permeation of a small molecule (glucose) and a large particle (LDL) through normal CEA tissue has been measured at room (20 °C) and physiological (37 ° C) temperatures using OCT. The permeation of glucose did not change significantly when the temperature was elevated from 20 °C to 37 °C, suggesting that the tissue is freely permeable to small molecules over this temperature range. In contrast, the permeation of LDL increased almost 2-fold with this temperature elevation, suggesting that this increase alters the structure of the arterial intima in a way that allows it to become much more permeable to large particles on the order of 20 nm in diameter. Unexpectedly, at 37 °C the permeation of LDL was 1.3-fold greater than that of glucose, suggesting that at this physiological temperature the movement of LDL across the intimal boundary is enhanced by an active mechanism in addition to passive diffusion. This study describes a new approach for quantitative measurement of lipoprotein movement into the subintimal space where multiple processes causing progression and regression of atherosclerosis occur.

Acknowledgments

This study was funded in part by grants from Office of Naval Research, The Institute of Biomedical Imaging Sciences, University of Houston Small Grants Program, and National Institutes of Health (HL 63090).

Abbreviations

OCT	optical coherence tomography
OCTSS	OCT signal slope
LDL	low density lipoprotein
HDL	high density lipoprotein
PBS	phosphate buffered saline
CEA	carotid endarterectomy

References

1. Lee AJ, Fowkes FG, Carson MN, Leng GC, Allan PL. European heart journal. 1997; 18:671–676. [PubMed: 9129900]

2. Patane S, Marte F, Sturiale M, Grassi R, Patane F. International journal of cardiology. 2009
3. Szmitko PE, Wang CH, Weisel RD, de Almeida JR, Anderson TJ, Verma S. Circulation. 2003; 108:1917–1923. [PubMed: 14568885]
4. Falk E. Journal of the American College of Cardiology. 2006; 47:C7–C12. [PubMed: 16631513]
5. Friedman MH, Fry DL. Atherosclerosis. 1993; 104:189–194. [PubMed: 8141842]
6. Tarbell JM. Annual review of biomedical engineering. 2003; 5:79–118.
7. Berliner JA, Navab M, Fogelman AM, Frank JS, Demer LL, Edwards PA, Watson AD, Lusis AJ. Circulation. 1995; 91:2488–2496. [PubMed: 7729036]
8. Genina EA, Bashkatov AN, Sinichkin YuP, Tuchin VV. Quantum Electronics. 2006; 36:1119–1124.
9. Kim H, Lizak MJ, Tansey G, Csaky KG, Robinson MR, Yuan P, Wang NS, Lutz RJ. Ann Biomed Eng. 2005; 33:150–164. [PubMed: 15771269]
10. Li SK, Jeong EK, Hastings MS. Investigative ophthalmology & visual science. 2004; 45:1224–1231. [PubMed: 15037591]
11. Bommannan D, Okuyama H, Stauffer P, Guy RH. Pharm Res. 1992; 9:559–564. [PubMed: 1495903]
12. Zysk AM, Nguyen FT, Oldenburg AL, Marks DL, Boppart SA. J Biomed Opt. 2007; 12 051403.
13. Stifter D. Applied Physics B: Lasers and Optics. 2007; 88:337–357.
14. Tomlins PH, Wang RK. Journal of Physics D: Applied Physics. 2005; 38:2519–2535.
15. Bouma, BE.; Tearney, GJ. Handbook of Optical Coherence Tomography. New York, NY: Marcel Dekker; 2002.
16. Brezinski, ME. Optical coherence tomography : principles and applications. Amsterdam ; Boston: Academic Press; 2006.
17. Ghosn MG, Carbajal EF, Befrui NA, Tellez A, Granada JF, Larin KV. Journal of biomedical optics. 2008; 13 010505.
18. Ghosn MG, Carbajal EF, Befrui NA, Tuchin VV, Larin KV. Journal of biomedical optics. 2008; 13 021110.
19. Ghosn MG, Tuchin VV, Larin KV. Optics letters. 2006; 31:2314–2316. [PubMed: 16832470]
20. Ghosn MG, Tuchin VV, Larin KV. Investigative ophthalmology & visual science. 2007; 48:2726–2733. [PubMed: 17525205]
21. Larin KV, Ghosn MG. Quantum Electronics. 2006; 36:1083–1088.
22. Larin KV, Ghosn MG, Ivers SN, Tellez A, Granada JF. laser physics letters. 2007; 4:312–317.
23. Larin KV, Tuchin VV. Quantum Electronics. 2008; 38:551–556.
24. Nelson, GJ. Blood lipids and lipoproteins: quantitation, composition, and metabolism. New York: Wiley-Interscience; 1972.
25. Esenaliev RO, Larin KV, Larina IV, Motamedi M. Optics letters. 2001; 26:992–994. [PubMed: 18040511]
26. Larin KV, Eledrisi MS, Motamedi M, Esenaliev RO. Diabetes care. 2002; 25:2263–2267. [PubMed: 12453971]
27. Renkin EM. Circulation research. 1977; 41:735–743. [PubMed: 923024]
28. Ghosn MG, Carbajal EF, Befrui NA, Tuchin VV, Larin KV. Optics and Lasers in Engineering. 2008; 46:911–914.
29. Park JH, Lee JW, Kim YC, Prausnitz MR. International journal of pharmaceutics. 2008; 359:94–103. [PubMed: 18455889]
30. Nielsen LB. Atherosclerosis. 1996; 123:1–15. [PubMed: 8782833]
31. Vasile E, Simionescu M, Simionescu N. The Journal of cell biology. 1983; 96:1677–1689. [PubMed: 6853599]
32. Rutledge JC. The American journal of physiology. 1992; 262:H234–H245. [PubMed: 1733315]
33. Larin KV, Motamedi M, Ashitkov TV, Esenaliev RO. Phys Med Biol. 2003; 48:1371–1390. [PubMed: 12812453]
34. Tuchin, VV. Optical Clearing of Tissues and Blood. Bellingham, WA: SPIE Press; 2005.

35. Tuchin VV, Maksimova IL, Zimnyakov DA, Kon IL, Mavlutov AH, Mishin AA. J. Biomed. Opt. 1997; 2:401–417. [PubMed: 23014964]
36. Yeh AT, Hirshburg J. Journal of biomedical optics. 2006; 11 014003.

Biographies

Kirill V. Larin, Ph.D. is Assistant Professor of Biomedical Engineering at the University of Houston, Houston, TX. His research interests focuses on development and application of OCT for noninvasive and nondestructive imaging and diagnostics of tissues and cells. Larin has authored more than 30 peer-reviewed journal publications and chapters in two textbooks on Biomedical Optics. He is recipient of Boris Yeltsin Presidential Award, Wallace Coulter Young Investigator Translation Award, Office of Naval Research Young Investigator Award, and Outstanding Young Investigator Award from the Houston Society for Engineers in Medicine and Biology.

Joel D. Morrisett, Ph.D. is Professor of Medicine and Biochemistry/Molecular Biology at Baylor College of Medicine, Houston, TX. His laboratory research has focused on the structure and function of lipids, lipoproteins, and lipid-metabolizing enzymes. His clinical research has been directed toward imaging of atherosclerosis by MRI.

Mohamad G. Ghosn is a Ph.D. candidate in the Biomedical Engineering program at the University of Houston. His main focus is the examination of molecular diffusion of various drugs and analytes across biological tissues using optical coherence tomography. He has had the opportunity to publish many of his works and he also enjoys teaching for which he was awarded the Outstanding Teacher Assistant Award for the year 2008 from the Cullen College of Engineering. His career goal is to become a professor in biomedical engineering.

Michael Leba is a senior undergraduate student majoring in Biomedical Engineering at the University of Houston. He has been involved in different projects involving optical imaging at the Biomedical Optics Laboratory. Michael plans to continue his graduate studies in the field of Biomedical engineering.

Astha Vijayananda is a junior undergraduate student majoring in Biomedical Engineering at the University of Houston. She is part of the Biomedical Optics Laboratory and is interested in research geared towards optical imaging. Her main focus in the laboratory is monitoring and quantifying molecular diffusion of biological tissues using optical coherence tomography. Her future goals are to attain Master's and Doctoral degrees in Biomedical Engineering and to devote her career to biomedical research.

As an undergraduate researcher in the Biomedical Optics Laboratory, Panteha Rezaee has focused her research on diffusion studies through tissues using optical imaging systems. She is finishing her third year in biomedical engineering and her interest in biomedical research has led her to plan to pursue a Master's degree in biomedical engineering. She wishes to be able to develop new and improve medical imaging technologies in the future.

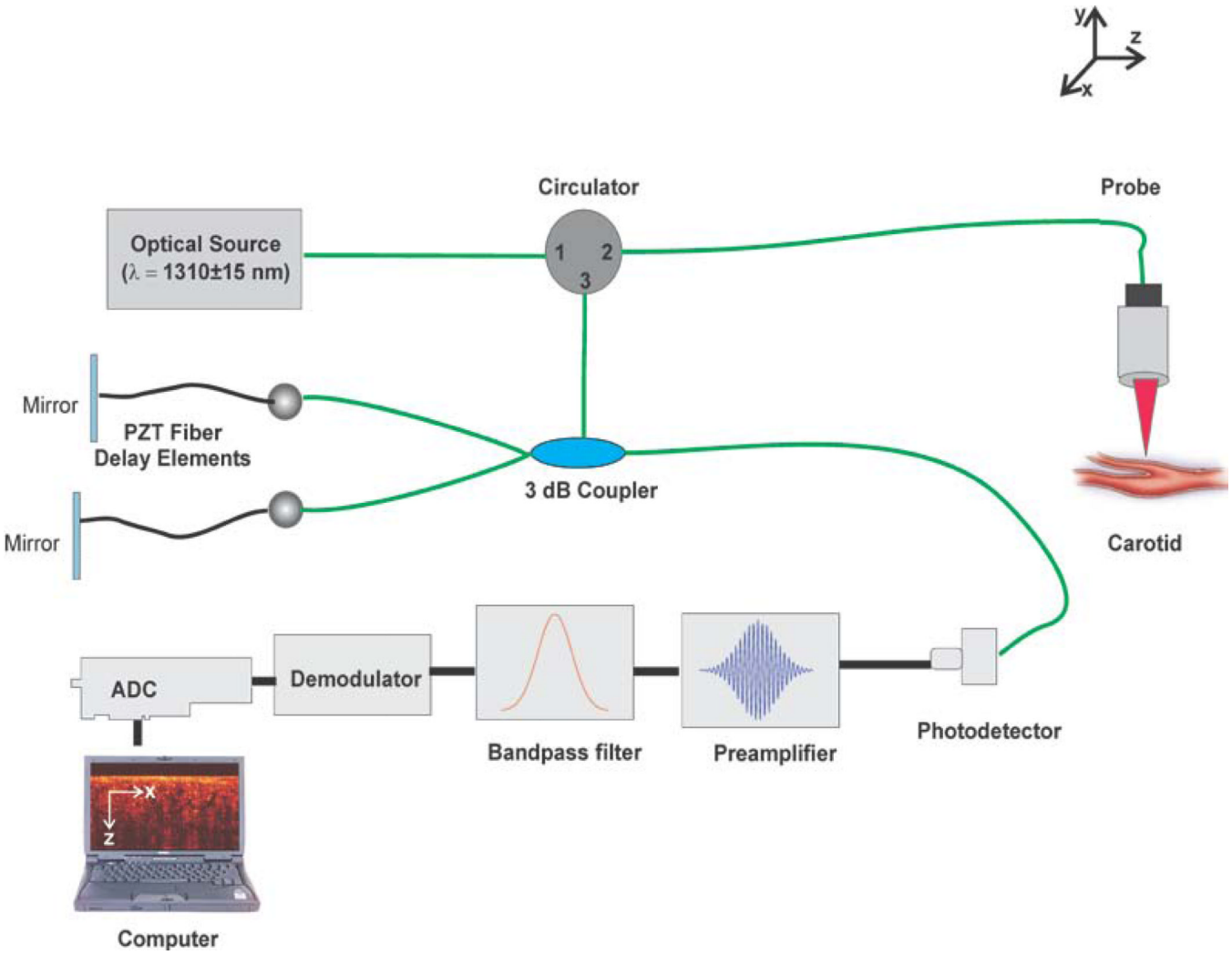

Figure 1.
Schematic of the Time-Domain OCT setup used to image carotid endarterectomy tissues.

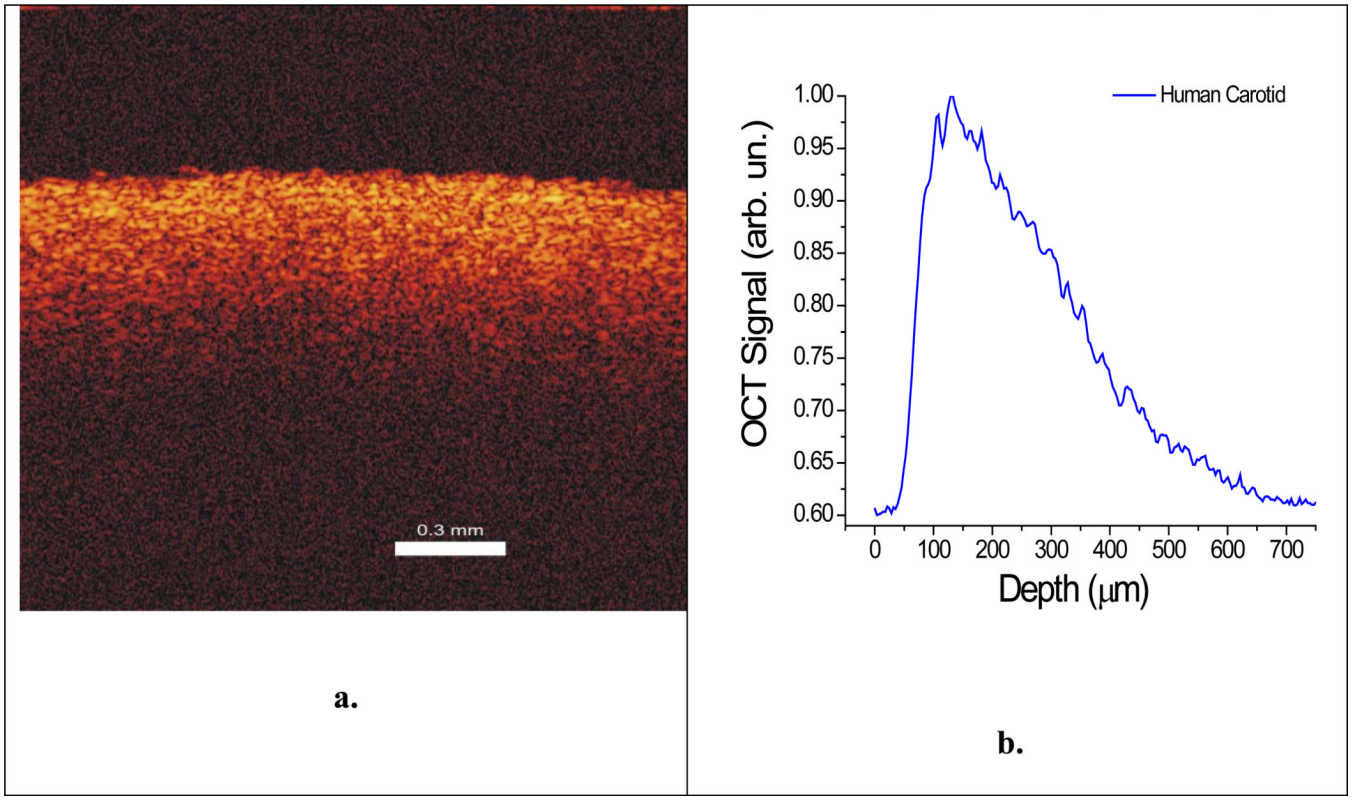

Figure 2.
(a) 2-dimensional image created by the OCT system and (b) 1-dimensional graph of the human carotid tissue obtained from the lateral averaging of the 2D image from (a).

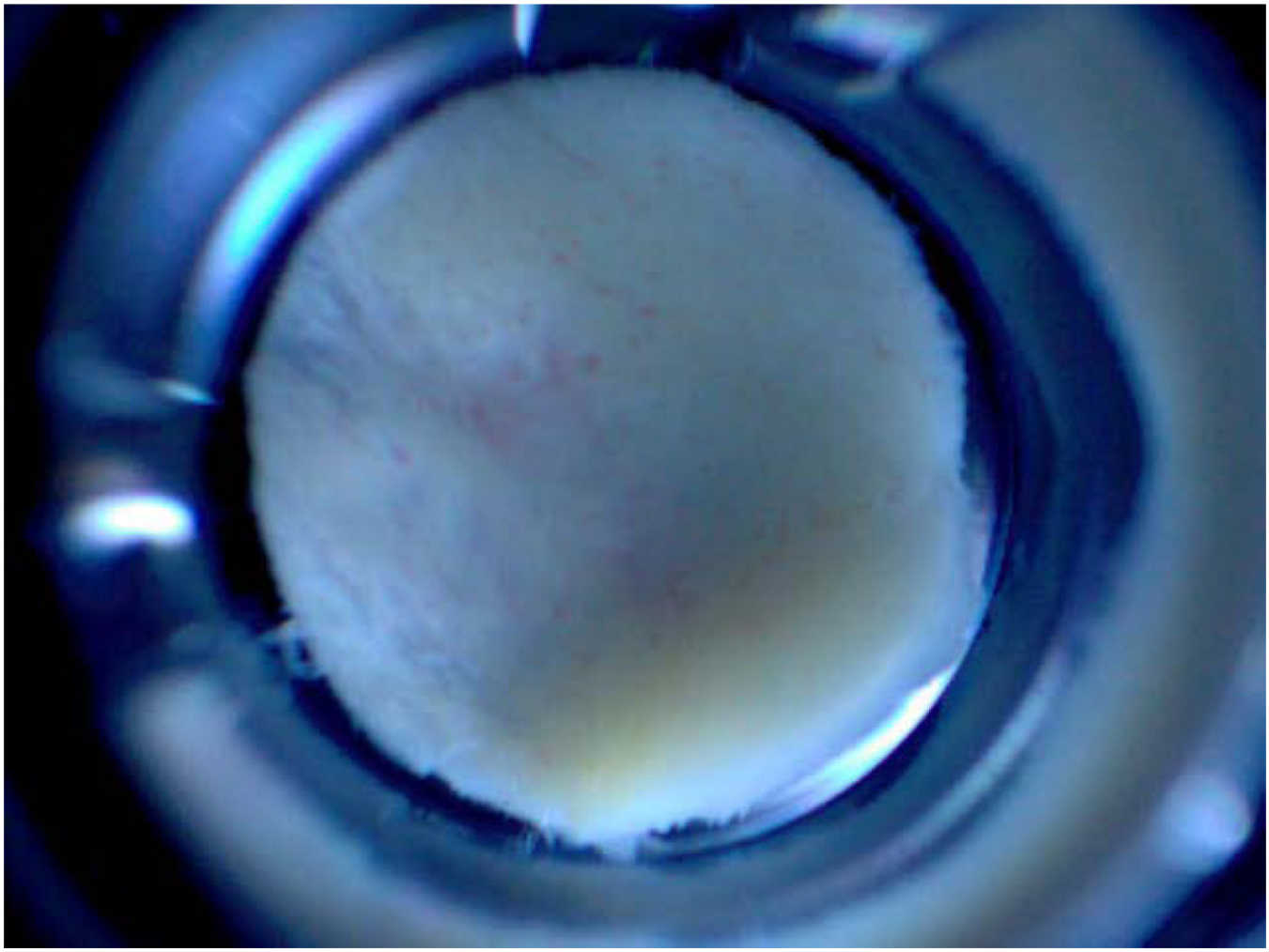

Figure 3.
Magnified photograph of a 5mm diameter carotid tissue sample immersed in PBS buffer in a well of a 96-well microtitre plate.

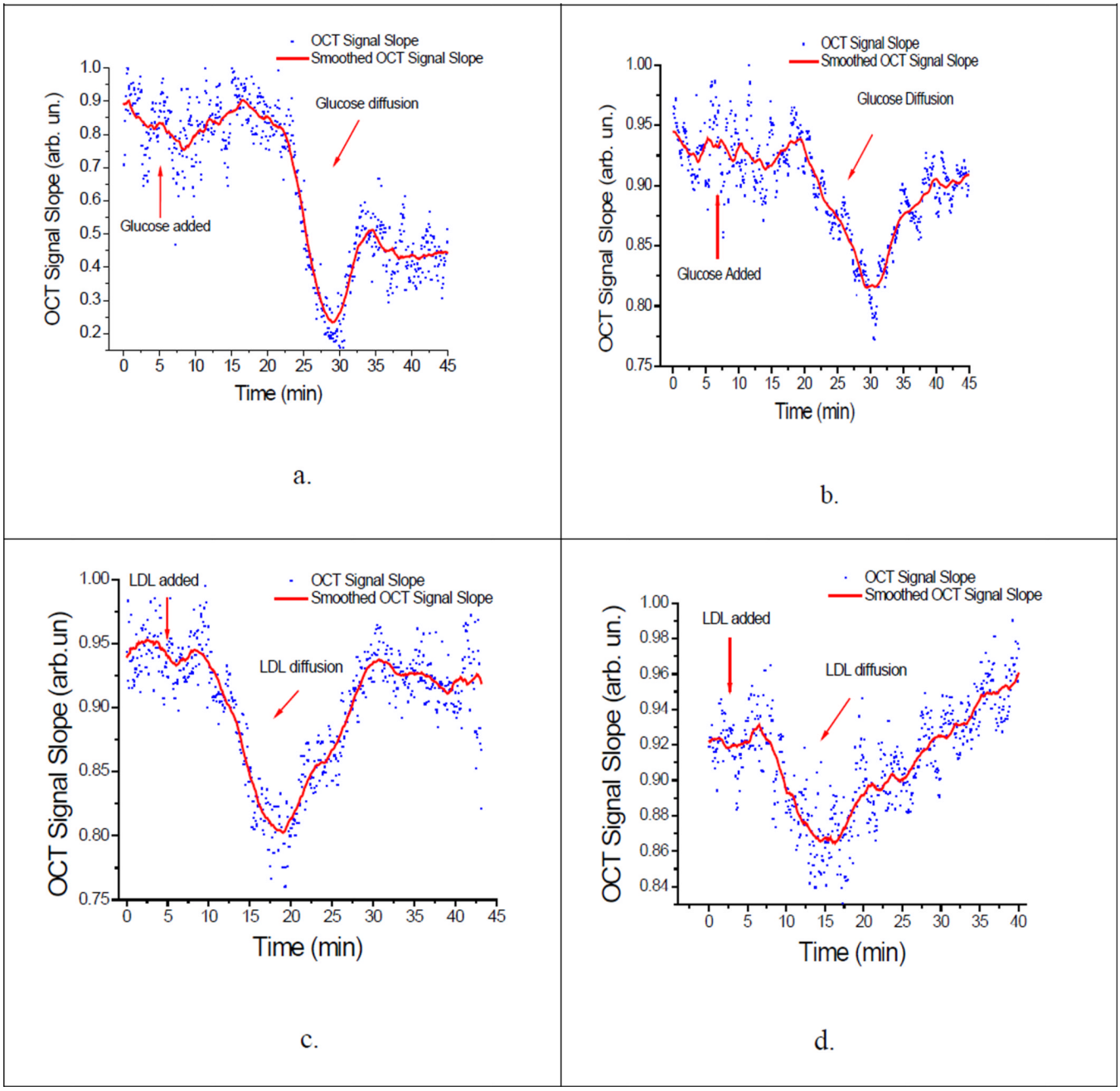

Figure 4.

OCTSS graphs of permeating species. (a) Glucose at 20°C, (b) Glucose at 37°C; (c) LDL at 20°C; (d) LDL at 37 °C) Dots represent the slope of the 1D graph in a chosen region over time. The graph is then smoothed per 50 points for clarity.

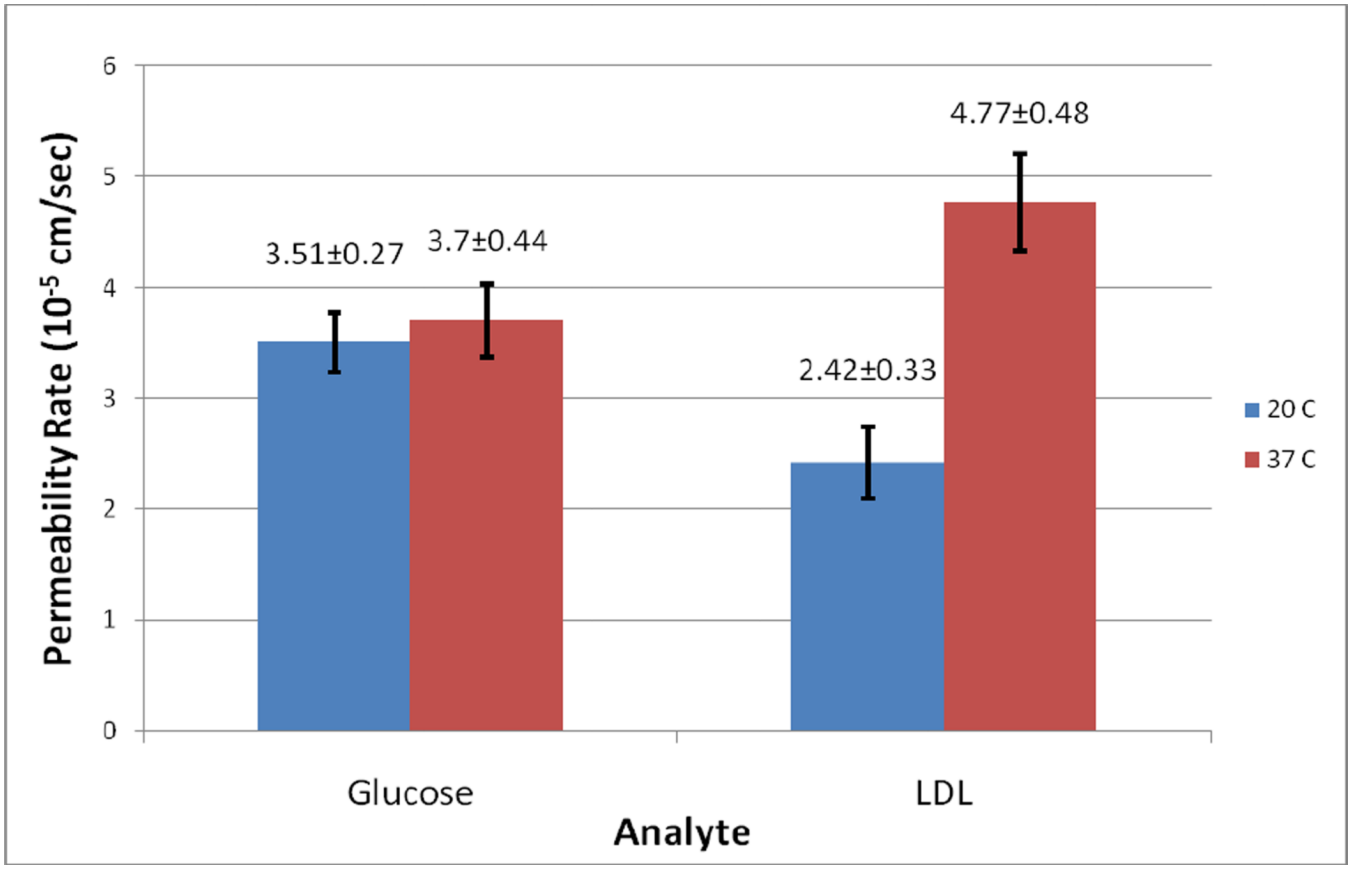

Figure 5.
The permeability rate of Glucose and LDL at 20 °C and 37°C in human carotid endarterectomy tissue.